V International Conference on Computational Methods in Marine Engineering
MARINE 2011
L. Eça, E. Oñate, J. Garca, P. Bergan and T. Kvamsdal (Eds)

NUMERICAL SIMULATION OF EXTREME WAVE IMPACT ON OFFSHORE PLATFORMS AND COASTAL CONSTRUCTIONS

ROEL LUPPES*, BULENT DUZ†, HENRI J.L. VAN DER HEIDEN*, PETER VAN DER PLAS* AND ARTHUR E.P. VELDMAN*

* Institute for Mathematics and Computer Science
University of Groningen
P.O. Box 407, 9700 AK Groningen, The Netherlands
e-mail: r.luppes@rug.nl, h.j.l.van.der.heiden@rug.nl, p.van.der.plas@rug.nl,
a.e.p.veldman@rug.nl

† Department of Ship Hydrodynamics
Technical University of Delft
Mekelweg 2, 2628 CD Delft, The Netherlands
e-mail: b.duz@tudelft.nl

Key words: Wave Impact, VOF, GABC, Regularisation, Local Grid Refinement

Abstract. The simulation tool ComFLOW, developed for accurate predictions of hydrodynamic wave loading, is based on the Navier-Stokes equations. The free-surface dynamics is described through VOF, with local height-function approach to enhance accuracy. Numerical reflections are prevented by specially designed absorbing boundary conditions. Gravity-consistent density averaging for two-phase flow prevents spurious velocities near the free surface. Good progress has been made in the prediction of sloshing, green water loading and wave run-up. In the ComFLOW3 project the focus is on wave propagation, the effect of viscosity in shear layers (regularisation turbulence modelling), interactive vessel-wave dynamics and improved numerical efficiency through local grid refinement.

1 INTRODUCTION

The hydrodynamic wave loading on structures plays an important role in coastal protection and the design of offshore constructions. Extreme waves and their impact loading can be a serious threat to the land behind dikes and the safety on and operability of offshore vessels. Recent tsunami flood waves (Indonesia 2004, Japan 2011) created huge devastations. The same holds for the big waves resulting from hurricanes that e.g. regularly ravage the Gulf of Mexico, with damage both on land and at sea. Also heavy internal sloshing may lead to serious problems, in the worst case even to capsize of e.g. a LNG carrier. Hence, a better understanding of wave impact forces is urgently needed.

Figure 1: Examples of damage because of extreme wave impact.

The CFD simulation tool ComFLOW has been developed for the accurate prediction of hydrodynamic wave loading on offshore and coastal protection structures, up to a detailed level[1–16]. For example, maximum pressure forces, duration of pressure peaks and shear stresses can be computed everywhere on a structure. The development is supported by several offshore-related companies (oil companies, ship yards, classification institutions, engineering companies), which are actively using ComFLOW for their activities.

In extreme wave loading events, the important physical phenomena are highly non-linear and dispersive. Hence, numerical tools based on simplified (potential flow, shallow-water) models only have limited applicability. ComFLOW solves the full Navier-Stokes equations in both water and air, with 2nd-order accuracy in both space and time, and the water surface is advected with high accuracy. Compressibility of the air can be included, which is especially important in cases of violent flow conditions, when air entrapment occurs. This basically makes ComFLOW able to accurately predict wave impact forces.

Good progress has been made in the prediction of flow phenomena such as sloshing, green water loading and wave run-up. In earlier MARINE conferences the numerical methods and progress in the ComFLOW development have been reported[3,7,10]. However, several aspects in the numerical model need further extension and improvement. In the ComFLOW3 project, improvement is aimed with respect to extreme waves and their propagation (model the oncoming waves until impact), viscous effects in shear layers (model small-scale flow details through regularisation turbulence modelling) and interactive vessel-wave dynamics (include coupling of wave and vessel motion). Besides this enlarged functionality, the numerical efficiency will be improved by means of local grid refinement techniques. In this paper, first a view scientific highlights of previous projects are discussed. Then first results of the ComFLOW3 project are presented.

2 PREVIOUS SCIENTIFIC HIGHLIGHTS

2.1 Accurate free-surface displacement

ComFLOW has been developed initially to study sloshing fuel on board spacecraft in micro-gravity, for which a very accurate and robust description of the free surface is required[5,17]. Later, the methodology was extended to simulations of sloshing liquids and two-phase flow in offshore applications, such as green water loading[1,2,5], impact loads on fixed structures[1,3–6,10,12] and sloshing tanks[7–9,13].

ComFLOW solves the Navier-Stokes equations in both water and air, with 2nd-order accuracy in both space and time, by means of 2nd-order upwind discretisation in combination with Adams-Bashforth time-stepping. The water surface is advected by means of a modified Volume-of-Fluid (VOF) method, with improved accuracy through a local height-function (LHF) approach, as described below. The employed numerical methods make ComFLOW suitable for accurate predictions of wave impact forces.

The Cartesian grid in ComFLOW provides a simple geometrical framework in which the position and slope of the free surface can be accurately described. On unstructured grids free-surface reconstruction is more difficult. Usually smearing of the free surface is needed, resulting in a 'spongy' surface. This will erroneously reduce peak pressures during impact and hence lead to less accurate wave-force predictions on unstructured grids.

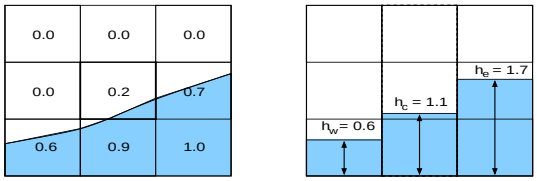

Figure 2: Construction of the LHF around a central S-cell by summing F_s values vertically.

The LHF is applied in a 3×3 block (3×3×3 in 3D) of cells surrounding a Surface-cell. First, the orientation of the free surface is determined (horizontal or vertical), depending on the filling rates F_s in the surrounding block of cells. Next, the horizontal or vertical height in each row or column is computed by summing F_s values, see Fig. 2. Based on the LHF, fluid is transported from one cell (donor) to another (acceptor), depending on the magnitude of local velocity, time step and grid sizes. Hence, the interface is explicitly reconstructed through a LHF and subsequently advected. The new interface is then reconstructed by means of another LHF, which ensures a sharp interface without smearing. As depicted in Fig. 3, the LHF approach results in significantly less loose droplets. Moreover, the LHF method is strictly mass conserving[1,5,8,9,17]. These are two improvements of unfavourable numerical artefacts of the original VOF method.

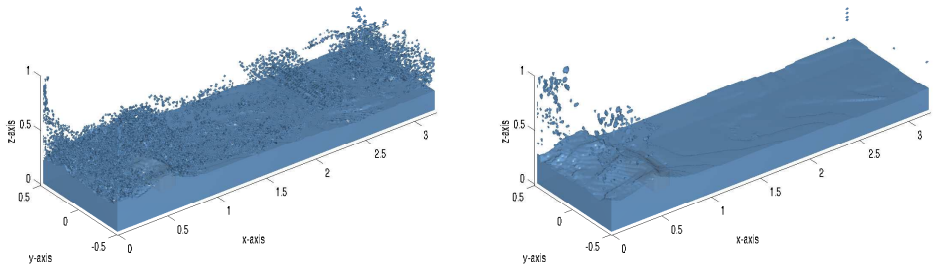

Figure 3: Liquid configuration after a dambreak simulation without (left) and with LHF (right). The LHF approach results in significantly less erroneous droplets.

2.2 Gravity-consistent density averaging

In case of two-phase flow, the discrete treatment of the density ρ near the free surface is important. Because of the staggered locations of variables around a computational cell, ρ is required at velocity locations (cell edges $i+\frac{1}{2}$), but is defined at cell centres, as indicated in Fig. 4. Simple geometrical averaging may result in spurious velocities, especially in case of high density ratios, and eventually cause severe instabilities near the free surface. In most of the literature, the spurious currents are damped with some form of diffusion or other suppression techniques, but in ComFLOW a much better technique is employed.

A superior averaging technique can be deduced by considering the momentum equation for a fluid at rest (hydrostatic conditions, zero velocities). This reduces to $\nabla p = \rho\vec{F}$ and hence $0 = \mathrm{curl}(\rho\vec{F})$, with $\vec{F}$ a body force. This condition should also hold for the discrete variables, otherwise velocity terms in the momentum equation no longer vanish and consequently spurious velocities are generated. This leads to a requirement how ρ should be averaged, as described below. Formulas for ρ that satisfy the requirement are called 'gravity consistent', as normally $\vec{F}$ includes gravity.

The naive geometrical average $(\rho_i + \rho_{i+1})/2$ is not gravity consistent. A gravity-consistent average is found by looking at the momentum control volume (the red-dashed region in Fig. 4) and weight the neighbouring density values with the fraction that this control volume is split by the free surface[7–9,15]. The different results when employing simple or gravity-consistent averaging are shown in Fig. 5 and Fig. 6.

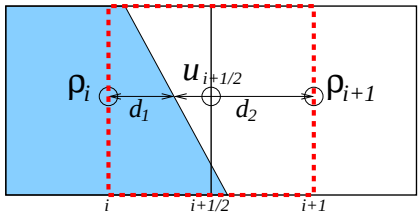

$$\rho_{i+\frac{1}{2}} = \frac{d_1\rho_{i+1} + d_2\rho_i}{d_1 + d_2}$$

Figure 4: The gravity-consistent density average $\rho_{i+1/2}$ is found by weighting ρ_i and ρ_{i+1} with the fraction (coefficients d_1 and d_2) that the free surface splits the red-dashed momentum control volume.

2.3 Generating and absorbing boundary conditions (GABC)

For simulations with open boundaries, a GABC has been designed that suppresses numerical wave reflections for a broad range of wave numbers. As a result, open boundaries can be located relatively close to a structure, without influencing outgoing waves or generating numerical reflections that affect water waves inside the flow domain. At the same time, regular or irregular waves can enter the flow domain as prescribed. Compared to traditional damping-zone techniques, less grid-points are required and computing times are reduced considerably[10–12].

The Sommerfeld condition for a potential Φ, $\left(\frac{\partial}{\partial t} + c^{out}\frac{\partial}{\partial x}\right)\Phi^{out} = 0$, is fully absorbing for one single outgoing wave component (phase velocity c^{out}) but gives reflections for

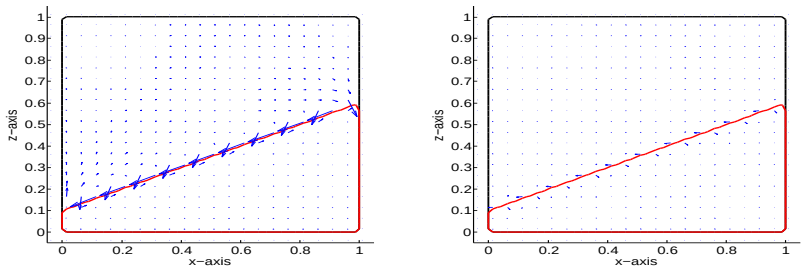

Figure 5: A hydrostatic case, with gravity perpendicular to the free surface. Simple geometrical averaging leads to spurious velocities (left). With gravity-consistent averaging, the free surface stays at rest (right).

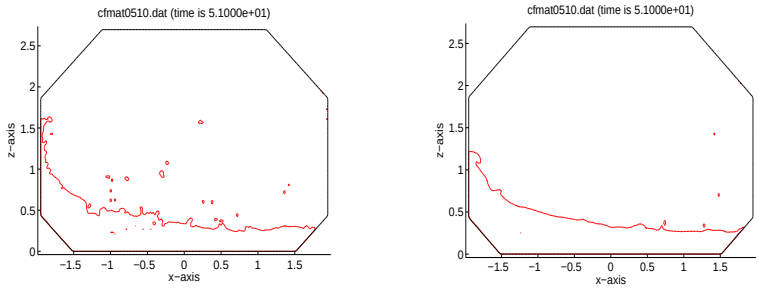

Figure 6: Liquid configuration after simulation of a sloshing experiment. With gravity-consistent density averaging (right), less instabilities are observed than with simple geometrical averaging (left).

waves composed of components with other phase velocities $c(kh)$. Instead of the constant approximation $c{=}c^{out}$, for the GABC the dispersion relation is approximated by

$$c = \sqrt{gh}\sqrt{\tanh(kh)}\,/\,\sqrt{kh} \approx \sqrt{gh}\frac{a_0 + a_1(kh)^2}{1 + b_1(kh)^2}, \tag{1}$$

where the coefficients a_0,a_1,b_1 are tuned for an optimal approximation over a large range of kh-values. Because of the e^{-kz}-behaviour of Φ, i.e. $k^2\Phi^{out} = \frac{\partial^2}{\partial z^2}\Phi^{out}$, k is replaced by 2nd-order derivatives along the boundary, thus leading to

$$\left[\left(1{+}b_1h^2\frac{\partial^2}{\partial z^2}\right)\frac{\partial}{\partial t} + \sqrt{gh}\left(a_0{+}a_1h^2\frac{\partial^2}{\partial z^2}\right)\frac{\partial}{\partial x}\right]\Phi^{out}{=}0. \tag{2}$$

With (2), reflection coefficients are significantly smaller over a wide range of the dimensionless wave number kh, than when Sommerfeld is used as boundary condition[10–12].

The derivatives of the potential in (2) are formally replaced through $\frac{\partial}{\partial x}\Phi{=}u$ and the Bernoulli equation $\frac{\partial}{\partial t}\Phi = -p - gz$. The momentum equation is used to eliminate the velocity at the new time instant u^{n+1}, which originates from $\frac{\partial}{\partial t}$. Boundary condition (2) is implemented numerically at the outflow boundary, which coincides with the location of the horizontal velocity u in an outflow cell. In this way spurious reflections are prevented, but interpolation over the boundary is required. The final result is a boundary condition for the pressure p. It is easily combined with the internal pressure Poisson equation, but has a larger stencil. Hence, the Poisson equation has to be solved by means of a powerful Krylov subspace method with incomplete LU preconditioning for acceleration.

3 NEW DEVELOPMENTS AND FUTURE PLANS

For more accurate predictions of hydrodynamic wave loading on offshore and coastal protection structures, in the ComFLOW3 project the focus is on extreme waves (and their propagation), the effect of viscosity in shear layers (regularisation turbulence modelling) and interactive vessel-wave dynamics. The numerical efficiency will be improved by means of local grid refinement. First results of the ComFLOW3 project are discussed in this section, together with future plans.

3.1 GABC extensions

The GABC, designed to minimise numerical reflections from open boundaries, has already been demonstrated for 2D waves propagating perpendicular to the open boundary[10–12]. As a first step, the GABC has been extended to waves entering the domain under an angle and leaving in different directions, as depicted in Fig. 7(left). For the latter, the GABC described in Section 2.3 has been modified by including direction cosines. Various tests indicate that differences between numerical results and analytical wave profiles are small or modest, for any incoming angle, and for a wide range of wave types. To study wave impact on a structure, ComFLOW users now have two possibilities: keep the position of the structure fixed and vary the angle α of the incoming wave, or rotate the structure and keep α constant. Moreover, the ComFLOW user can cut-off the domain at all boundaries, which saves computing time. The reflection can be measured from the differences between the small and large domain in Fig. 7(right). For an incoming 5th-order Stokes wave under a 45^o angle, with wave period $7.5s$ and height $1.3m$, the observed difference is below 2% up to 17s simulation time. Further details can be found in[14,16].

In the future, the GABC will be made more suitable for non-linear and extreme waves and the effects of stationary currents will be included. A more accurate GABC will be implemented, based on an extension of Sommerfeld, viz. the 2nd-order Higdon condition

$$\prod_{j=1}^{2} \left(\frac{\partial}{\partial t} + c_j \frac{\partial}{\partial x} \right) \Phi = 0, \tag{3}$$

which obviously will also include direction cosines. With (3), a fair range in incidence angles can be covered, without leading to serious implementation complexity. However, the Poisson matrix does become more complex and probably a dedicated Poisson solver is needed for computational efficiency.

3.2 Regularisation modelling of viscous effects

There are many practical (offshore) applications where viscosity is significant, often in combination with wave effects. Examples are side-by-side mooring, sloshing in moon pools, scouring and vortex shedding behind structures. For an accurate prediction of hydrodynamic forces and resistance due to viscous effects, a careful treatment of viscous wall and free shear flow is required. At least the large-scale viscous flow effects should

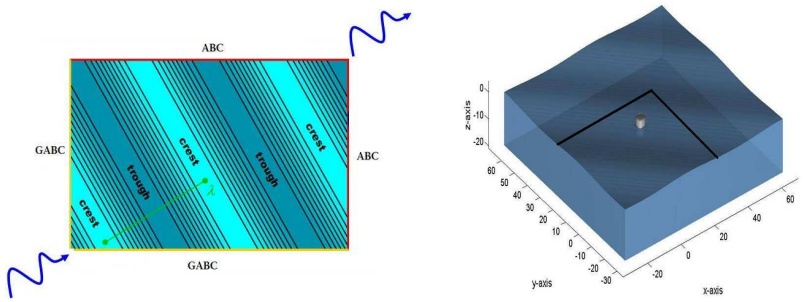

Figure 7: Schematic picture of GABC possibilities (left). All outflow boundaries can be taken close to the structure (right), which saves computing time.

be described accurately. As viscous effects originate from the structure, the discretisation of diffusion near solid walls has been improved. In ComFLOW, a cut-cell approach is used to describe a solid geometry, where apertures describe cell volume or face ratios that are open for flow. The discretisation of shear stresses ($\frac{\partial}{\partial y}u, \frac{\partial}{\partial x}v$, etc.) has been refined, making careful use of aperture information following the LS-STAG method[18]. Normal stresses ($\frac{\partial}{\partial x}u, \frac{\partial}{\partial y}v, \frac{\partial}{\partial z}w$) are discretised analogous to pressure gradients. In 3D roughly 100 cut-cell cases have to be considered, which however can be found largely by rotating a few basic cases. Already for simple test cases as 2D Poiseuille flow ($\frac{\partial^2}{\partial y^2}u$ and $\frac{\partial}{\partial x}p$ constant) the improvement is clear: analytical profiles are more accurately simulated.

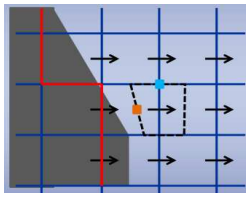

Figure 8: The LS-STAG discretisation of momentum diffusion is based on the deformed momentum control volume (dashed region), making careful use of aperture information.

In many practical applications, turbulence is responsible for a wide range of scales of motion. The required resolution for the smaller scales would lead to excessive computing times. Therefore, in ComFLOW an 'energy-preserving' turbulence model is implemented, which gives an accurate description of the large scale flow effects, even on coarse grids. The production of small scales is controlled by a special treatment of the convection term, instead of adding eddy-viscosity[19]. It is consistent with the energy-preserving discretisation methods[20] that are already employed in ComFLOW.

The convection term $C(u,u)$ in the Navier-Stokes equations is responsible for the creation of small scales. The regularisation approach modifies this term to restrain this production. A symmetric self-adjoint filter is used to filter the scales below a certain threshold. This leads to a 2nd-order (in filter length) accurate approximation of the convection term $C_2(u,u) = \overline{C(\overline{u},\overline{u})}$, where the bar means application of the filter. The great

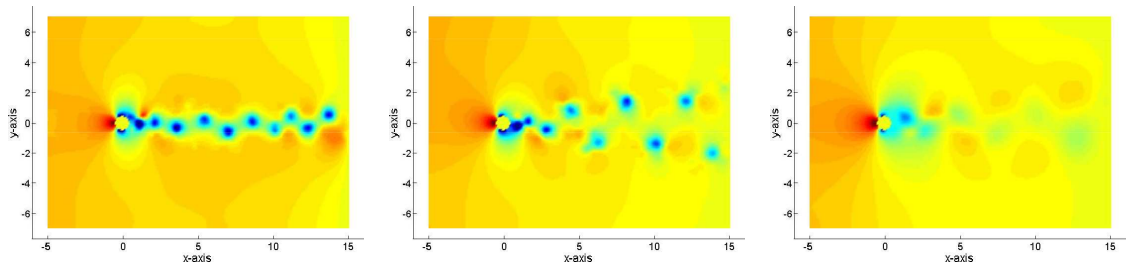

Figure 9: The pressure field during vortex shedding behind a circular cylinder, with pure central discretisation (left), central discretisation with C_2 regularisation (middle) and upwind discretisation (right).

virtue of this model is that it conserves the same important physical quantities as the original convection term, viz. energy, enstrophy and helicity. Especially energy conservation is crucial for correct prediction of large scale flow. Currently, simple explicit filters are used, e.g. in 1D $\overline{u_i} = \omega^2(u_{i+1} + u_{i-1}) + (1 - 2\omega^2)u_i$, with ω proportional to the filter length. The correct implementation and type of filter are still subject of study.

As a test case, the vortex shedding behind a circular cylinder is studied (Re=2000), for 3 different treatments of convection. Close examination of the velocity field shows that with pure central discretisation there are wiggles (numerical artefact) in front of the cylinder and in the vortex region behind. The application of C_2 reduces wiggles, but small 'wrinkles' are observed in the velocity field, which requires further investigation. Because of the additional numerical diffusion, in the upwind simulation wiggles are fully suppressed. However, pressure peaks and troughs are not properly predicted, the vortex street is too wide and the additional numerical diffusion results in an overshoot of drag force. The C_2 simulation gives the most realistic wake prediction, as shown in Fig. 9.

In the future, the improved discretisation near solid walls will be investigated further. It will be combined with C_2 regularisation. The near-wall modelling (influence of turbulent boundary layer) will be improved as well. And obviously the turbulence near the free-surface has to be described accurately for a good prediction of hydrodynamic wave loading.

3.3 Improved numerical efficiency

To facilitate practical simulations of ComFLOW with large numbers of computational cells (up to 50 million in the near future), the numerical efficiency has to be increased. One approach is to divide computations over multiple cores (parallelisation). ComFLOW uses an explicit time-stepping procedure. At every time step the pressure has to be computed, the velocity field has to be updated and the free-surface has to be advected. Solving the pressure is the far most time-consuming part (up to 95% of the total time). Hence, first parallelisation actions concerned the pressure Poisson solver and also faster Poisson solvers are investigated. With the GABC the computational domain can be decreased effectively, which saves grid points. Extension of its applicability and performance are subject of study. Moreover, with regularisation turbulence models computing time is saved, because of the lower need for grid resolution in comparison with LES/RANS models.

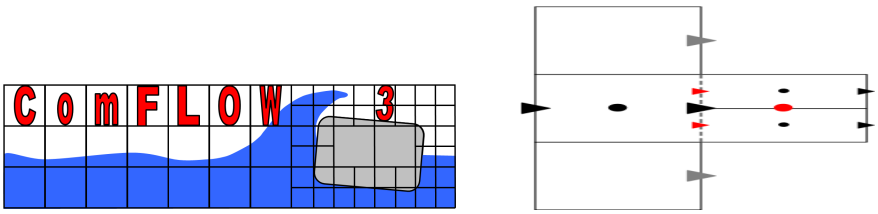

Figure 10: LGR in the ComFLOW3 logo: near the structure cells are split with a 1:2 ratio (left). Discretisation near the refinement (right) involves known (black/grey) and virtual variables (red).

Another way to increase the numerical efficiency is using local grid refinement (LGR). For the prediction of hydrodynamic pressure loads on structures, generally a high grid resolution is required near the structure. Further away, in the less interesting parts of the flow domain, a coarser mesh is usually sufficient. Overall grid stretching leads to cells with unfavourable large aspect ratios and therefore in certain parts of the domain cells are split into finer cells (see Fig. 10, left). As a first step, the data structure in ComFLOW has been modified, by adding an additional index l to the cell indices (i, j, k), indicating the refinement level. In this way, each cell of the coarse base grid (indicated by $l=0$) can be divided into finer cells ($l=1$), which can also be split-up ($l=2$), etc. By making clever use of pointers, all existing subroutines can be used without modification. Only for the layers where the actual refinement takes place new subroutines are required, containing e.g. the discretisation of the momentum equations over the 1:2 refinement boundary.

For the discretisation near a grid refinement, special attention is required for the locations of variables. While setting up the discretised Poisson equation, coarse velocities are placed at the interface. The velocity u and pressure gradient $\frac{\partial}{\partial x}p$ are taken constant on the coarse cell face, similar to the ideas presented in[21]. Missing variables (see Fig. 10, right) are found from interpolation. As a result, a compact scheme is found for the pressure equation, with 1st-order accuracy. Simple tests with Couette flow ($\frac{\partial}{\partial y}u$ and p constant) and Poiseuille flow ($\frac{\partial^2}{\partial y^2}u$ and $\frac{\partial}{\partial x}p$ constant) revealed that errors are generally very small. Only at subgrid corners little deviation from the analytical solutions is found, which will be investigated further in the future. In Fig. 11, the flow around a circular cylinder is considered, with two levels of grid refinement near the cylinder. The snapshots of pressure and vorticity show that the flow goes through the refinement layers without disturbance.

In the future, advection of the free surface through refinement boundaries will be investigated. The displacement algorithm will have to be adjusted to the local changes in grid structure. Moving objects will be subject of study as well. They will have to move through refinement areas without deformation.

3.4 Interactive body motion (IBM)

The first application of IBM with ComFLOW was the interaction between internal liquid sloshing and overall spacecraft dynamics. Experiments in space with the Sloshsat FLEVO satellite were supported by ComFLOW simulations[5,17] (see Fig. 12, left). The

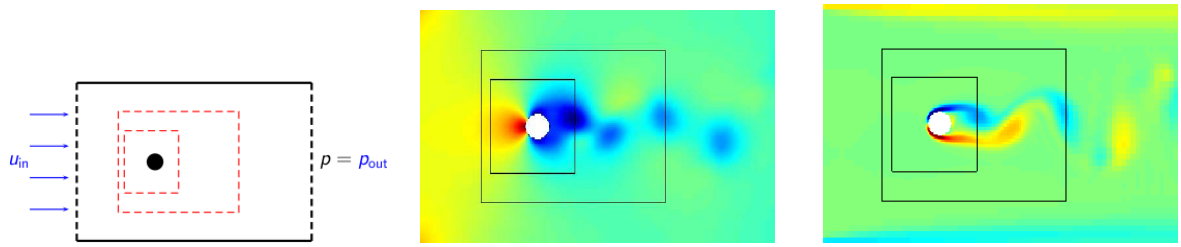

Figure 11: Local grid refinement for the flow around a circular cylinder ($D = 1\,m$, $U_{in} = 1.0\,m/s$, $Re = 100$). Schematic overview of setup (left), computed pressure distribution (middle) and vorticity (right).

Navier-Stokes equations for the fluid and the equations for solid-body dynamics were directly coupled and solved simultaneously. The influence of the moving fluid was accounted for by computing the variable centre of mass, moment of inertia and (pressure and viscous) forces on the tank wall every time step. Another example of IBM with ComFLOW is the simulation of the Statoil Snorre tension leg platform[22] (see Fig. 12, right), where the mechanical motion algorithm and the flow solver were also strongly intertwined.

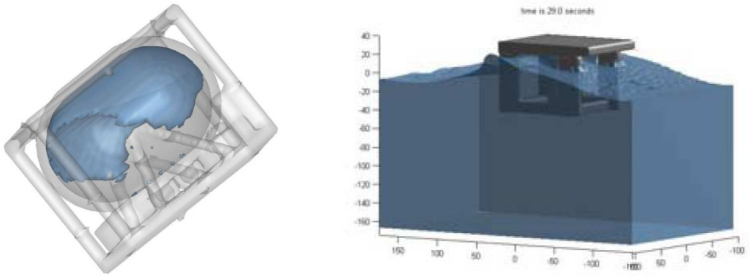

Figure 12: Examples of IBM studies with ComFLOW. Interaction between internal sloshing and overall spacecraft dynamics (Sloshsat FLEVO, left). Interaction between water waves and mechanical anchor constructions (Statoil Snorre TLP, right).

Unfortunately, direct coupling is not always possible, e.g. when one of the solvers is part of a commercial code (black box). However, a strong coupling is usually required for stability in case of large mass and inertia ratios. In ComFLOW, the quasi-simultaneous approach will be implemented[23]. In this method, a simple approximation of the mechanical model is implemented as a preconditioner, to enhance convergence of the iterations between fluid and body. This provides sufficient stability of the coupling, also when the exact dynamical model is applied in the second step.

4 CONCLUSION

The CFD simulation tool ComFLOW has been developed for the accurate prediction of hydrodynamic wave loading on offshore and coastal protection structures. Over the years, several numerical techniques have been developed using ComFLOW. A number of proven techniques have been presented: absorbing boundary conditions to minimise

numerical reflections from open boundaries, local height function for accurate free-surface displacement and gravity-consistent density averaging for two-phase flow to prevent spurious velocities near the free surface. Also several first steps and future plans to enlarge the functionality of ComFLOW have been discussed. The GABC has been extended for incoming and outgoing waves under an angle. The effect of viscosity in shear layers is more accurately described through regularisation turbulence modelling and improved diffusion discretisation. With local grid refinement the numerical efficiency has been increased.

In the future the focus is on extreme waves (and their propagation) and further improvement of both regularisation modelling and local grid refinement. Also interactive vessel-wave dynamics will be subject of study.

Acknowledgement

The research is supported by the Dutch Technology Foundation STW, applied science division of NWO and the technology program of the Ministry of Economic Affairs in The Netherlands (contracts GWI.6433 and 10475).

REFERENCES

[1] Kleefsman, K.M.T., Fekken, G., Veldman, A.E.P., Iwanowski, B. and Buchner, B. A Volume Of Fluid Based Simulation Method for Wave Impact Problems. *J. Comp. Phys.*, 206(1):363–393, 2005.

[2] Kleefsman, K.M.T., Loots, G.E., Veldman, A.E.P., Buchner, B., Bunnik, T. and Falkenberg, E. The numerical solution of green water loading including vessel motions and the incoming wave field. In *24th Int. Conf.*, 2005. OMAE2005-67448.

[3] Veldman, A.E.P., Kleefsman, K.M.T. and Fekken, G. Numerical computation of wave impact. In *Int. Conf.*, pages 323–332, 2005. MARINE 2005.

[4] Wemmenhove, R., Loots, G.E., Luppes, R. and Veldman, A.E.P. Modeling two-phase flow with offshore applications. In *24th Int. Conf.*, 2005. OMAE2005-67460.

[5] Veldman, A.E.P. The simulation of violent free-surface dynamics at sea and in space. In *Eur. Conf.* ECCOMAS CFD, 2006. ISBN 909020970-0, paper 492.

[6] Wemmenhove, R., Loots, G.E. and Veldman, A.E.P. Hydrodynamic wave loading on offshore structures simulated by a two-phase flow model. In *25th Int. Conf.*, 2006. OMAE2006-92253.

[7] Wemmenhove, R., Luppes, R., Veldman, A.E.P. and Bunnik, T. Numerical simulation and model experiments of sloshing in LNG tanks. In *Int. Conf.*, 2007. MARINE 2007.

[8] Wemmenhove, R., Luppes, R., Veldman, A.E.P. and Bunnik, T. Application of a VOF Method to Model Compressible Two-Phase Flow in Sloshing Tanks. In *27th Int. Conf.*, 2008. OMAE2008-57254.

[9] Luppes, R., Wemmenhove, R., Veldman, A.E.P. and Bunnik, T. Compressible Two-Phase Flow in Sloshing Tanks. In *5th Eur. Congr.* ECCOMAS, 2008.

[10] Luppes, R., Wellens, P.R., Veldman, A.E.P. and Bunnik, T. CFD simulations of wave run-up against a semi-submersible with absorbing boundary conditions. In *Int. Conf.*, 2009. MARINE 2009.

[11] Wellens, P.R., Luppes, R., Veldman, A.E.P. and Borsboom, M.J.A. CFD simulations of a semi-submersible with absorbing boundary conditions. In *28th Int. Conf.*, 2009. OMAE2009-79342.

[12] Luppes, R., Veldman, A.E.P. and Wellens, P.R. Absorbing Boundary Conditions for Wave Simulations around Offshore Structures. In *Eur. Conf.* ECCOMAS CFD, 2010.

[13] Luppes, R., Veldman, A.E.P. and Wemmenhove, R. Simulation of two-phase flow in sloshing tanks. In *Computational Fluid Dynamics 2010*, pages 555–561. ICCFD, 2010. ISBN: 9783642178832.

[14] Duz, B., Huijsmans, R.H.M., Wellens, P.R., Borsboom, M.J.A. and Veldman, A.E.P. Towards a general-purpose open boundary condition for wave simulations. In *30th Int. Conf.*, 2011. OMAE2011-49979.

[15] Veldman, A.E.P., Luppes, R., Bunnik, T., Huijsmans, R.H.M., Duz, B., Iwanowski, B., Wemmenhove, R., Borsboom, M.J.A., Wellens, P.R., van der Heiden, H.J.L. and van der Plas, P. Extreme wave impact on offshore platforms and coastal constructions. In *30th Int. Conf.*, 2011. OMAE2011-49488.

[16] Duz, B., Huijsmans, R.H.M., Veldman, A.E.P., Borsboom, M.J.A. and Wellens, P.R. An absorbing boundary condition for regular and irregular wave simulations. In *Int. Conf.*, 2011. MARINE 2011.

[17] Veldman, A.E.P., Gerrits, J., Luppes, R., Helder, J.A. and Vreeburg, J.P.B. The numerical simulation of liquid sloshing on board spacecraft. *J. Comp. Phys.*, 224:82–99, 2007.

[18] Cheny, Y. and Botella, O. The LS-STAG method: A new immersed boundary/level-set method for the computation of incompressible viscous flows in complex moving geometries with good conservation properties. *J. Comp. Phys.*, 229:1043–1076, 2010.

[19] Verstappen, R.W.C.P. On restraining the production of small scales of motion in a turbulent channel flow. *Comp. Fluids*, 37:887–897, 2008.

[20] Verstappen, R.W.C.P. and Veldman, A.E.P. Symmetry-Preserving Discretisation of Turbulent Flow. *J. Comp. Phys.*, 187:343–368, 2003.

[21] Uzgoren, E., Singh, R., Sim, J. and Shyy, W. Computational modeling for multiphase flows with spacecraft application. *Progr. in Aerospace Sc.*, 43(4-6):138–192, 2007.

[22] Johannessen, T.B., Haver, S., Bunnik, T. and Buchner, B. Extreme wave effects on deep water TLP's. In *Proc. Deep Offshore Techn. 2006*, 2006.

[23] Veldman, A.E.P. A simple interaction law for viscous-inviscid interaction. *J. Eng. Math.*, 65:367–383, 2009.